REVISTA ÁGUAS SUBTERRÂNEAS

Investigation of aquifer vulnerability to pollution using index Based-Models within Okigwe South, Imo State, Nigeria

Investigação da vulnerabilidade do aquífero à poluição utilizando modelos baseados em índices em Okigwe Sul, Estado de Imo, Nigéria

Jude Maduabuchi Anyanwu[1], Daniel Nnaemeka Obiora[2], Desmond Okechukwu Ugbor[3], Johnson Cletus Ibuot[4], James Obinna Sampson[5]

[1]University of Nigeria – Nigeria, judeanyanwu25@gmail.com
[2]University of Nigeria – Nigeria, daniel.obiora@unn.edu.ng
[3]University of Nigeria – Nigeria, desmond.ugbor@unn.edu.ng
[4]University of Nigeria – Nigeria, johnson.ibuot@unn.edu.ng
[5]University of Nigeria – Nigeria, obinnae25@gmail.com

Received:
January 24, 2026
Received in revised form:
March 9, 2026
Accepted:
March 9, 2026
Available online:
June 23, 2026
Section:
Articles

Keywords:
Aquifer Vulnerability.
Groundwater Pollution.
Index-Based Models.
Groundwater Protection.

Palavras-chave:
Vulnerabilidade de aquíferos.
Poluição de águas subterrânea.
Modelos baseados em índices.
Proteção de águas subterrâneas.

https://doi.org/10.14295/ras.v40i2.30395

ABSTRACT

Groundwater is the primary source of potable water in Okigwe South, southeastern Nigeria, yet increasing anthropogenic activities pose significant contamination risks to the underlying aquifers. This study integrated geophysical, hydrogeological, and hydrochemical approaches to assess aquifer vulnerability and groundwater quality in the area. A total of 50 Vertical Electrical Sounding (VES) surveys using the Schlumberger configuration and 8 groundwater samples were collected across Ehime-Mbano, Ihitte/Uboma, and Obowo Local Government Areas. Aquifer vulnerability was evaluated using the Aquifer Vulnerability Index (AVI), DRASTIC, and SINTACS models, while groundwater quality was assessed using the Water Quality Index (WQI). Geo-electrical parameters derived from VES data were used to characterize subsurface lithology and estimate hydraulic properties of protective layers. Spatial analysis and contour map generation were carried out using Python-based scripts for interpolation and visualization. The results indicate moderate to very high aquifer vulnerability, particularly within Obowo LGA, largely controlled by shallow water table conditions, permeable sandy lithologies, and thin vadose zones. WQI results reveal groundwater quality ranging from good to very poor, with zones of degraded quality correlating well with areas of high vulnerability identified by the index-based models. The integration of geophysical and hydrochemical data enhances confidence in vulnerability assessment and provides a robust framework for groundwater protection planning. The generated vulnerability and water quality maps offer valuable tools for sustainable groundwater management and regulatory decision-making in Okigwe South.

RESUMO

A água subterrânea é a principal fonte de água potável em Okigwe South, no sudeste da Nigéria, porém as crescentes atividades antropogênicas representam riscos significativos de contaminação aos aquíferos subjacentes. Este estudo integrou abordagens geofísicas, hidrogeológicas e hidroquímicas para avaliar a vulnerabilidade do aquífero e a qualidade da água subterrânea na região. Um total de 50 levantamentos elétricos verticais (VES) utilizando a configuração de Schlumberger e 8 amostras de água subterrânea foram coletados nas Áreas de Governo Local de Ehime-Mbano, Ihitte/Uboma e Obowo. A vulnerabilidade do aquífero foi avaliada utilizando os modelos Índice de Vulnerabilidade do Aquífero (AVI), DRASTIC e SINTACS, enquanto a qualidade da água subterrânea foi avaliada pelo Índice de Qualidade da Água (WQI). Parâmetros geoelétricos derivados dos dados de VES foram utilizados para caracterizar a litologia subsuperficial e estimar as propriedades hidráulicas das camadas de proteção. A análise espacial e a geração de mapas de contorno foram realizadas utilizando scripts em Python para interpolação e visualização. Os resultados indicam vulnerabilidade do aquífero de moderada a muito alta, particularmente na LGA de Obowo, controlada principalmente por condições de lençol freático raso, litologias arenosas permeáveis e zonas vadosas finas. Os resultados do WQI revelam qualidade da água subterrânea variando de boa a muito ruim, com zonas de qualidade degradada correlacionando-se bem com áreas de alta vulnerabilidade identificadas pelos modelos baseados em índices. A integração de dados geofísicos e hidroquímicos aumenta a confiabilidade da avaliação de vulnerabilidade e fornece uma estrutura robusta para o planejamento da proteção da água subterrânea. Os mapas gerados de vulnerabilidade e qualidade da água oferecem ferramentas valiosas para a gestão sustentável da água subterrânea e para a tomada de decisões regulatórias em Okigwe South.

1. INTRODUCTION

Aquifer vulnerability evaluation assesses the degree to which groundwater systems are susceptible to contamination due to natural hydrogeological conditions and anthropogenic pressures. This assessment integrates factors such as aquifer lithology, soil characteristics, and thickness of the unsaturated zone, recharge conditions, and the physicochemical properties of potential contaminants (Foster, 1987; Aller et al., 1987; Vrba & Zaporozec, 1994). In the 21st century, increasing population growth, urban expansion, and intensified agricultural and industrial activities have placed unprecedented pressure on groundwater resources, making their protection a critical concern for public health and environmental sustainability. Numerous groundwater wells worldwide have been abandoned due to contamination resulting from the downward migration of pollutants through permeable subsurface layers, originating from sources such as septic systems, refuse dumps, hydrocarbon spills, and corrosion-related processes (Sampath, 2000).

Groundwater resources are intrinsically vulnerable to pollution because contaminants introduced at the surface can migrate through the vadose zone and reach aquifers, depending on lithological composition, hydraulic properties, and recharge dynamics. Intrinsic vulnerability reflects the natural sensitivity of an aquifer system to contamination, independent of specific pollutant types, and is governed by geological and hydrogeological characteristics (Vrba and Zaporozec, 1994). As emphasized by Agoubi et al. (2018), Rizka (2018), and George (2021a), vulnerability assessments are indispensable tools for identifying areas at risk, minimizing groundwater degradation, and guiding sustainable water resource management. This need is particularly acute in densely populated regions where groundwater is the primary source of domestic water supply and where unregulated drilling practices persist (Piver et al., 1997; Vu et al., 2021).

Over the past decades, several index-based approaches have been developed to quantify aquifer vulnerability. Among these, the DRASTIC model evaluates seven hydrogeological parameters: depth to the water table, net recharge, aquifer media, soil media, topography, impact of the vadose zone, and hydraulic conductivity (Aller et al., 1987). The SINTACS model applies similar parameters but offers greater flexibility through weighting schemes adapted to local hydrogeological conditions (Civita & De Maio, 2000). Other vulnerability assessment methods, 323including GOD (Foster, 1987), GODL (Foster & Hirata, 1988), AVI (Van Stempvoort et al., 1993), GLSI (Albinet & Margat, 1970), and longitudinal unit conductance (Henriet, 1976) approaches, have also been employed to evaluate aquifer vulnerability based on combinations of geological, hydrogeological, and geophysical parameters. In parallel, geophysical techniques—particularly vertical electrical sounding (VES)—have gained prominence due to their ability to characterize subsurface resistivity, layer thicknesses, and protective capacity of overburden materials, which are critical for evaluating aquifer susceptibility to contamination. Recent studies have demonstrated the effectiveness of integrating geophysical, hydrogeological, and hydrochemical approaches for groundwater vulnerability and quality assessment across diverse geological settings (Ahmed et al., 2022; Singh et al., 2023; Sharma et al., 2023).

Despite the widespread application of these models, most previous studies in southeastern Nigeria have applied single or limited vulnerability indices without systematically integrating geophysical, hydrogeological, and hydrochemical datasets for model validation and cross-comparison. Furthermore, the degree to which different vulnerability models converge or diverge in identifying high-risk zones remains insufficiently explored, particularly in sedimentary terrains characterized by variable lithology and intense anthropogenic activity. This lack of integrated assessment introduces uncertainty in vulnerability zoning and limits the reliability of groundwater protection strategies. The Okigwe South area of Imo State, including Obowo Local Government Area, is underlain by heterogeneous sedimentary formations and experiences increasing pressure from agricultural practices, waste disposal, and expanding rural settlements. Groundwater constitutes the primary source of potable water in this region, yet systematic assessments of aquifer vulnerability remain scarce. The presence of permeable sandy units interbedded with clay lenses, combined with shallow water table conditions in some locations, raises concerns regarding the potential for rapid contaminant migration into underlying aquifers.

In this context, the present study addresses a critical gap by integrating geophysical, hydrogeological, and hydrochemical approaches to provide a robust and comparative assessment of aquifer vulnerability in Okigwe South. Vertical electrical sounding (VES) data are combined with multiple index-based models—AVI, DRASTIC, and SINTACS—to evaluate intrinsic vulnerability, while water quality index (WQI) analysis is employed to assess

groundwater quality and validate vulnerability predictions. Unlike conventional single-model approaches, this integrated framework enables inter-model comparison, identification of model convergence and divergence, and improved confidence in vulnerability mapping.

The objectives of this study are to characterize subsurface lithology and aquifer protective capacity using vertical electrical sounding data; to assess intrinsic groundwater vulnerability using AVI, DRASTIC, and SINTACS models; to evaluate groundwater quality through water quality index (WQI) analysis; to compare and integrate vulnerability indices with hydrochemical results for model validation; and to delineate high-risk zones in order to provide scientifically grounded recommendations for groundwater protection and sustainable management in Okigwe South, southeastern Nigeria.

2. GEOGRAPHICAL AND GEOLOGICAL SETTING OF THE STUDY AREA

Okigwe South is located between latitudes 5.570°N and 5.700°N and longitudes 7.230°E and 7.380°E in southeastern Nigeria (Fig. 1). The area lies within the Anambra Basin, a major depocentre of clastic sediments in the southern segment of the Benue Trough, which has undergone complex tectono-sedimentary evolution (Oladimeji and Nwajide, 2022). Administratively, Okigwe South comprises Ehime-Mbano, Obowo, and Ihitte/Uboma Local Government Areas, where groundwater constitutes the principal source of potable water for domestic and agricultural use. Geologically, the area is underlain by sedimentary formations that exert strong control on groundwater occurrence, flow, and vulnerability. The Ajali Formation, which outcrops extensively in the region, is characterized by thick, friable, fine- to medium-grained sandstone units that are often iron-stained and highly permeable. These characteristics favor high groundwater storage and transmission but also increase susceptibility to contaminant infiltration. The Mamu and Nsukka formations, which overlie or laterally grade into the Ajali Formation, consist of alternating sandstone, shale, and coal seams, introducing heterogeneity in aquifer continuity and protective capacity.

In parts of the region, particularly toward the eastern flank, the Imo Formation is encountered and is composed predominantly of shale with thick clay horizons, bluish-grey ironstone, and thin, indurated sandstone bands containing molluscan fossils (Anyanwu and Oguntade, 2021). While the shale and clay units provide some degree of natural protection to underlying aquifers, lateral facies changes into sandstone—especially toward the eastern margin—reduce this protective capacity and enhance vertical percolation. The Imo Formation is considered laterally equivalent to the Ameki Group, which includes the Nanka Sand, Nsugbe Formation, and Ameki Formation (Nwajide, 1979; Whiteman, 1982), further emphasizing the lithological variability of the subsurface. Hydrogeologically, groundwater occurs mainly within the sandstone units of the Ajali and Ameki formations, where recharge is largely controlled by precipitation and infiltration through the overlying vadose zone. The coexistence of highly permeable sandy units and less permeable shale–clay layers results in spatially variable aquifer protective capacity, making parts of Okigwe South particularly sensitive to contamination. This vulnerability is further exacerbated by increasing anthropogenic activities such as agriculture, waste disposal, and rural settlement expansion, especially in Obowo Local Government Area, where organic pollution has been previously reported. The complex lithological architecture and contrasting hydrogeological properties of the formations underlying Okigwe South make the area suitable for integrated geophysical and index-based vulnerability assessment. Vertical electrical sounding (VES) provides an effective means of delineating subsurface layers, estimating overburden thickness, and evaluating aquifer protective capacity, which are critical inputs for vulnerability modeling in sedimentary terrains with limited borehole control.

3. METHODOLOGY AND MATERIALS

3.1. Ves-based geoelectrical survey

A systematic geophysical survey was conducted to delineate subsurface hydrogeological layers and assess aquifer protective capacity. Fifty Vertical Electrical Sounding (VES) surveys were carried out across strategically selected locations in Ihitte/Uboma, Ehime-Mbano, and Obowo LGAs (Fig. 3), ensuring coverage of major lithological units and variability in land use. Site selection considered uniform spacing, lithological heterogeneity, and proximity to potential contamination sources.

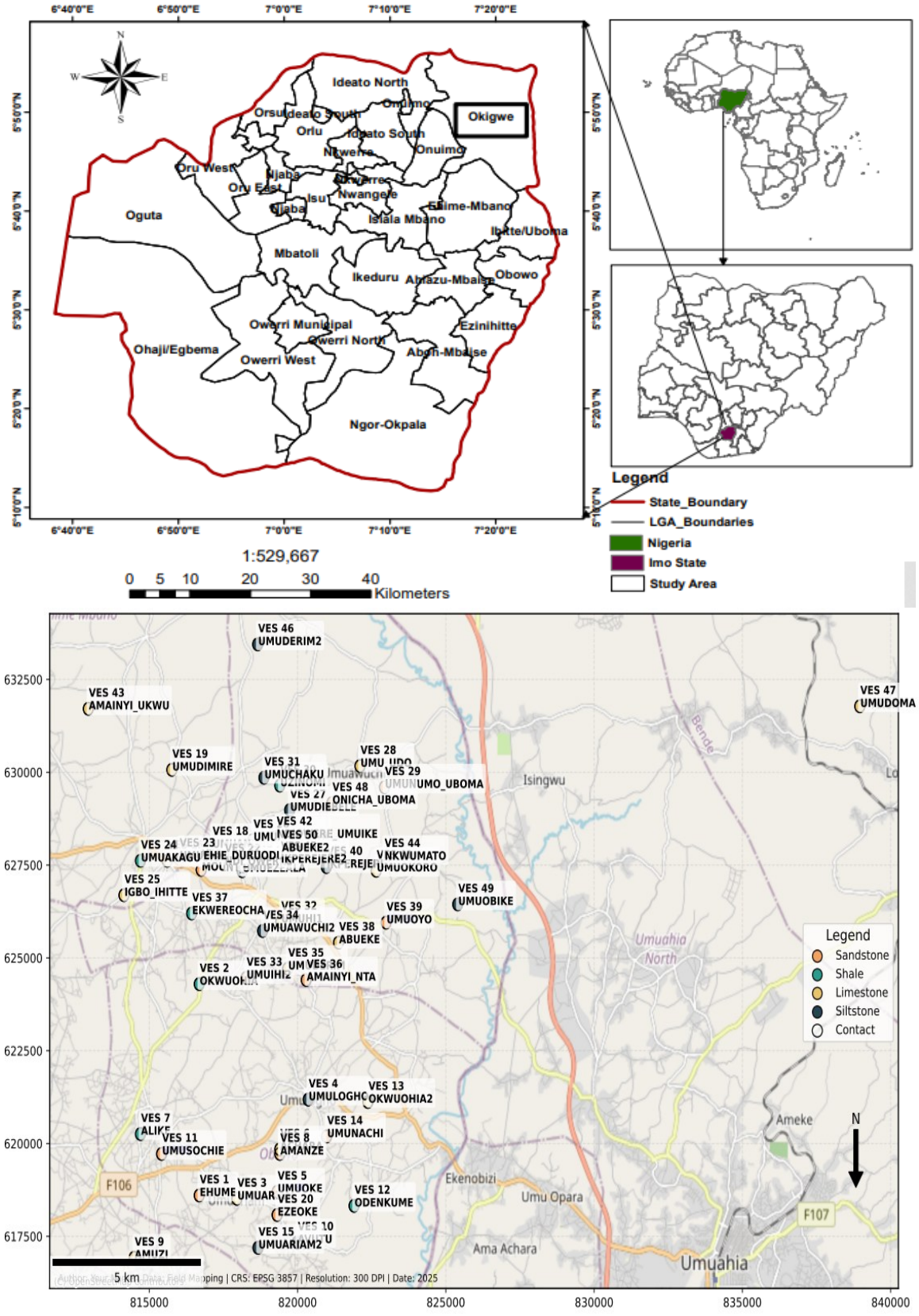

Figure 1. Location Map of the Study Area.

Field measurements were obtained using an Integrated Geo-Resistivity Meter (IGR), which consists of a current injection unit and a potential difference measurement system designed for resistivity surveys. The acquired field data were subsequently processed with the WINRESIST software package in order to determine true resistivity values, layer thicknesses, depths of investigation, and probable lithologic characteristics. The apparent resistivity (ρ_a) was calculated using the standard expression:

$$\rho_a = \pi \frac{\left(\frac{AB}{2}\right)^2 - \left(\frac{MN}{2}\right)^2}{MN} R_a \quad (1)$$

where AB is the current electrode separation, MN is the potential electrode separation, R_a is the apparent electrical resistance measured in the field. Equation 1 can be written as:

$$\rho_a = \mathrm{G}R_a \quad (2)$$

here G is the geometric factor given by:

$$\mathrm{G} = \pi \frac{\left(\frac{AB}{2}\right)^2 - \left(\frac{MN}{2}\right)^2}{MN} \quad (3)$$

The VES data were plotted on a bi-logarithmic graph, with apparent resistivity (ρ_a) plotted against AB/2 electrode spacings. To improve data quality, the resulting curves were refined by removing anomalous points that could increase the root mean square (rms) error (Ekanem; Udosen, 2023a, 2023b). After this refinement, any remaining variations observed within the curves were interpreted as genuine vertical or lateral changes in subsurface resistivity distribution. Figure 3 presents sample VES models generated by WINRESIST. The resulting geo-resistivity profiles of the subsurface are influenced by factors such as lithology, salinity, moisture content, material density, as well as the size, geometry, and connectivity of pores within the rock matrix.

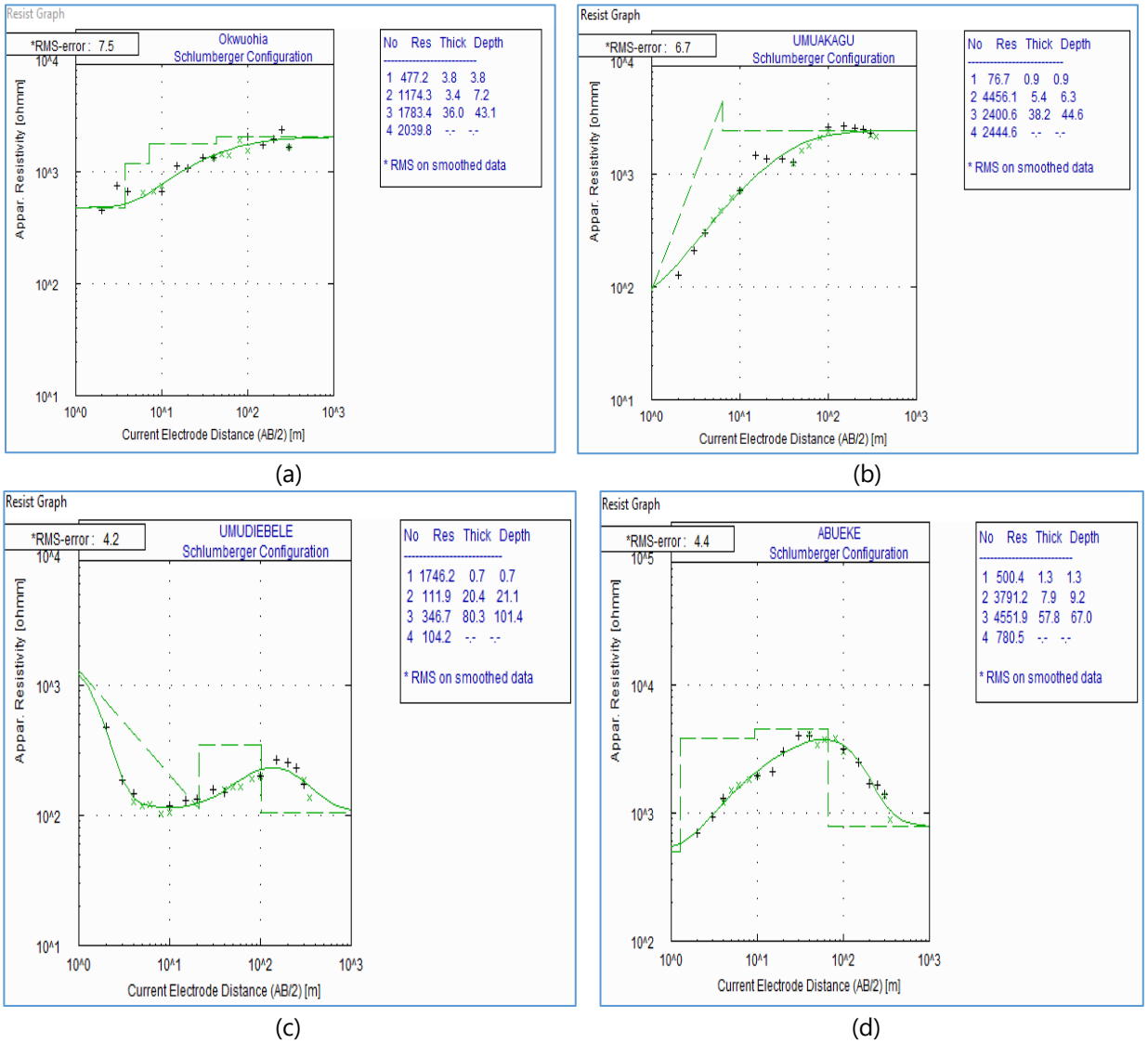

Figure 2 (a-d). Sample model inversion curves derived from surface resistivity survey data.

3.2. Aquifer vulnerability index (AVI)

The Aquifer Vulnerability Index (AVI) is a numerical method for assessing an aquifer's inherent susceptibility to contamination from surface sources. It focuses on the hydrogeological properties of overlying soils and geologic layers that act as natural protective barriers. As proposed by Van Stempvoort, Ewert and Wassenaar (1993), AVI quantifies vulnerability based on the vertical hydraulic resistance of these layers. Compared to the DRASTIC model, AVI often indicates higher vulnerability, especially in shallow aquifers (Ducci; Sellerino, 2013). The method uses two main parameters—the thickness (h) of protective layers and their hydraulic conductivity (K)—to calculate hydraulic resistance (C), expressed as:

$$C = \sum_{i=1}^{n} \frac{h_i}{K_i} \quad (4)$$

where K_i is the hydraulic conductivity, while h_i is the thickness of the vadose zone materials. AVI classes are assigned according to Table 1, with lower resistance corresponding to higher vulnerability.

Table 1 – Relationship between AVI and C (Van Stempvoort; Ewert; Wassenaar. 1993)

Hydraulic resistance (C)	Log C	Vulnerability (AVI)
0-10	< 1	Extremely high
10-100	1-2	High
100-1000	2-3	Moderate
1000–10,000	3-4	Low
> 10,000	> 4	Extremely low

3.3. Drastic

Groundwater vulnerability was also assessed using the DRASTIC model, which incorporates seven hydrogeological parameters: Depth to Water (D), Net Recharge (R), Aquifer Media (A), Soil Media (S), Topography (T), Impact of Vadose Zone (I), and Hydraulic Conductivity (C) (Aller *et al.*, 1987). Each parameter was rated and weighted according to standard guidelines (Table 2). The DRASTIC Index (DI) was calculated as:

$$\text{DRASTIC Index (DI)} = D_R D_W + R_R R_W + A_R A_W + S_R S_W + T_R T_W + I_R I_W + C_R C_W \quad (5)$$

where subscripts R and W denote rating and weight, respectively.

3.4. Sintacs

The SINTACS model (Civita, 1994) uses the same seven hydrogeological parameters as DRASTIC but applies modified weights to better reflect regional conditions (Awawdeh; Al Mahamid; Jaradat, 2020). Vulnerability scores were computed as:

$$\text{SINTACS Index (SI)} = S_r S_w + I_r I_w + N_r N_w + T_r T_w + A_r A_w + C_r C_w + S_r S_w \quad (6)$$

Tables 3 provide parameter ratings and weights used in this study. SINTACS is suitable for medium- to large-scale regional assessments and facilitates comparison with DRASTIC and AVI results.

3.5. Water Quality Index (AQI)

Groundwater quality was evaluated using the Water Quality Index (WQI), integrating multiple physico-chemical parameters to provide a single quality score (Brown *et al.*, 1970). Eight water samples were collected during the dry season (month/year) to minimize temporal variability. Parameters analyzed included pH, TDS,

major cations (Ca^{2+}, Mg^{2+}, Na^{+}, K^{+}), major anions (Cl^{-}, SO_4^{2-}, NO_3^{-}), and trace metals (if measured). WQI was calculated as:

$$\mathrm{WQI} = \frac{\sum(W_\mathrm{i} - Q_\mathrm{i})}{\sum W_\mathrm{i}} \tag{7}$$

where Q_i is the quality rating for parameter i, W_i is the assigned weight, and $\sum W_\mathrm{i}$ is the total weight. Classification followed Brown *et al.* (1970), as summarized in Table 4.

Table 2 – DRASTIC ratings and weighting for each parameter (Aller *et al.* 1987)

Parameter	Interval/Class	Rating(R)	Weight (W)
Depth to Water (m)	0–1	10	5
	1–4	9	5
	4–10	7	5
	10–20	5	5
	>20	3	5
Recharge (mm/yr)	>250	8	4
	100–250	6	4
	50–100	4	4
	<50	2	4
Aquifer Media	Clay	2	3
	Sandstone	6	3
	Sand & Gravel	8	3
Soil Media	Clay	1	2
	Loam	5	2
	Sand	9	2
Topography (Slope %)	0–2	10	1
	2–6	9	1
	6–12	5	1
	>12	3	1
Vadose Zone	Clay	3	5
	Sandstone	6	5
	Sand & Gravel	8	5
Hydraulic Conductivity (m/s)	$<1\times10^{-5}$	2	3
	$1\times10^{-5} – 1\times10^{-4}$	4	3
	$>1\times10^{-4}$	6	3

Table 3 – SINTACS ratings and weighting for each of the parameters Civita (1994)

Parameter	Symbol	Interval/Class	Rating (R)
Depth to water (m)	S	0–1.5	10
		1.5–4.5	9
		4.5–15	7
		15–30	3
		>30	1
Net Recharge (m)	I	>0.025	9
		0.01–0.025	6
		0–0.01	3
Aquifer Media	N	Clayey formations	2
		Sandstone /fractured rocks	6
		Sand & gravel / karst	8–10
Soil Media	T	Clay	1–3
		Loam	5
		Sandy loam	6
		Sand / gravel	9–10
Topography (slope %)	A	0–2	10
		2–6	9
		6–12	7
		>12	3–5

Table 3 – SINTACS ratings and weighting for each of the parameters Civita (1994) — Continued

Parameter	Symbol	Interval / Class	Rating (R)
Vadose Zone Impact	C	Clay	3
		Loam	5
		Sandstone	6
		Sand / gravel	8–10
Hydraulic Conductivity (m/s)	S	$>10^{-4}$	10
		10^{-5}– 10^{-4}	7–8
		10^{-6} – 10^{-5}	5–6
		$<10^{-6}$	1–3

Table 4 – WQI Parametric Range by Brown et al. (1970)

WQI Range	Water Quality
0 – 25	Excellent
26 – 50	Good
51 – 75	Poor
76 – 100	Very Poor
>100	Unsaturated for drinking

3.6. Integration of Geophysical and Hydrogeological Data

Subsurface resistivity and layer thicknesses derived from VES surveys were used to estimate the thickness and hydraulic conductivity of vadose zone materials, which served as key inputs for the AVI, DRASTIC, and SINTACS models. Spatial analyses, including contour map generation, interpolation, and comparison of DRASTIC and SINTACS index values, were performed using Python 3.10 with custom scripts developed for data processing, visualization, and overlay of vulnerability indices. This Python-based workflow enabled consistent and reproducible map generation, facilitated inter-model comparison, and allowed validation of vulnerability predictions against Water Quality Index (WQI) results. The approach ensured accurate identification of high-risk zones and supported quantitative assessment of aquifer vulnerability across the study area.

4. RESULTS AND DISCUSSION

4.1. Geo-electric sounding

Vertical Electrical Sounding (VES) was conducted at 50 locations using the Schlumberger array, with apparent resistivity plotted against half-current electrode spacing. Data were interpreted using Python (Spyder IDE) and WINRESIST software, which matched field curves with theoretical models to derive geo-electric parameters, following methods by Akpan, Ilori and Essien (2013) and Ibuot, George and Obiora (2013). Model fits were evaluated using RMSE, with lower values indicating better accuracy (George; Ibuot; Obiora, 2021). Primary parameters—resistivity and layer thickness—were extracted and used to calculate secondary indices for groundwater potential estimation (Bawallah *et al.*, 2018). Table 5 summarizes variations in resistivity, thickness, depth, and elevation, illustrating subsurface heterogeneity (Obianwu; Okeke; Onyekuru, 2011). The first layer resistivity (ρ_1), representing the topsoil, varies significantly: low values (e.g., 22.2 Ωm at VES 45 – IKPEREJERE II) suggest clayey or moist soils, while high values (e.g., 5276.1 Ωm at VES 20 – EZEOKE) indicate dry, sandy, or lateritic material. The second layer (ρ_2) reflects weathered or fractured zones; low resistivity (12.8 Ωm at VES 21 – UMUEZEALA) indicates saturated clay or silty soils, whereas high resistivity (11,928.4 Ωm at VES 16 – UMUAKAGU II) suggests dry sands or compact rock fragments. The third layer (ρ_3), often the main aquifer, shows extremely high resistivity at VES 16, 17, 23, 26, and 33 (10,000–31,000 Ωm), indicating dry or compact formations with limited water-bearing potential (Olayinka; Barker, 1990). The fourth layer (ρ_4), generally representing deeper basement rock, ranges from 12.5 to over 30,000 Ωm, reflecting lithological and moisture variability.

Layer thicknesses (h_1–h_3) also vary markedly. Thin upper layers (0.5 m at UMUAWUCHI II, 0.7 m at UMUEZEALA) indicate loose soils, while thick third layers (126.3 m at UMUARIAM II, 405.9 m at MOUNT OLIVE) suggest deep aquifers or bedrock. Depth to layers (d_1–d_3) ranges from 12.1 m (UMUNUMO-UBOMA) to 413.8 m (MOUNT OLIVE), critical for borehole planning and hydrogeological assessment. Elevations span 86.0–189.0 m, influencing runoff, infiltration, and groundwater flow.

Table 5 – Summary of Interpreted Vertical Electrical Sounding (VES) Data

VES	Location	Latitude (°N)	Longitude (°E)	Layer resistivity (Ωm)				Thickness (m)			Depth (m)			Elevation (m)	Curve Types
				ρ_1	ρ_2	ρ_3	ρ_4	h_1	h_2	h_3	d_1	d_2	d_3		
1	EHUME	5.5483	7.3364	1178.1	221.1	2926.7	2125.1	1.2	5.1	54.0	1.2	6.3	60.3	88.0	HK
2	OKWUOHIA	5.5992	7.3364	477.2	1174.3	1783.4	2039.8	3.8	3.4	36.0	3.8	7.2	43.1	111.0	AA
3	UMUARIAM	5.5475	7.3478	110.5	4538.2	119.0	2526.2	0.8	4.6	36.2	0.8	5.4	41.6	150.0	KH
4	UMULOGHO	5.5714	7.3694	350.5	987.3	5637.9	1452.7	4.5	3.0	32.1	4.5	7.5	39.6	99.0	AK
5	UMUOKE	5.5492	7.3600	1683.9	1139.6	245.0	1011.4	2.5	32.7	41.7	2.5	35.2	76.8	113.0	QH
6	ACHARA	5.5594	7.3608	201.4	37.8	158.5	518.7	3.6	6.8	52.5	3.6	10.4	62.9	86.0	HA
7	ALIKE	5.5631	7.3186	326.1	315.0	1338.1	4408.2	2.4	8.6	10.4	2.4	11.0	21.4	86.0	HA
8	AMANZE	5.5583	7.3608	67.5	1359.1	288.9	1170.0	2.5	7.4	32.2	2.5	10.0	42.1	172.0	KH
9	AMUZI	5.5333	7.3167	192.7	167.6	825.6	2611.4	4.7	13.2	24.5	4.7	17.9	42.4	98.0	HA
10	AVUTU	5.5370	7.3661	374.5	1318.4	3081.6	1177.7	2.6	20.6	71.1	2.6	23.2	94.3	101.0	AK
11	UMUSOCHIE	5.5583	7.3250	332.0	37.3	2285.4	1137.3	1.0	2.1	34.0	1.0	3.0	37.0	112.0	HK
12	ODENKUME	5.5458	7.3833	379.4	1275.8	934.3	1134.3	1.2	10.1	29.1	1.2	11.2	40.3	118.0	KH
13	OKWUOHIA II	5.5708	7.3875	307.2	51.4	278.4	2199.5	3.4	8.3	13.8	3.4	11.7	25.5	116.0	HA
14	UMUNACHI	5.5625	7.3750	172.7	627.1	6192.8	545.6	2.7	13.2	55.8	2.7	15.9	71.8	114.0	AK
15	UMUARIAM II	5.5357	7.3542	998.0	4228.7	2501.2	1230.2	3.6	10.2	126.3	3.6	13.9	140.2	117.0	KQ
16	UMUAKAGU II	5.6289	7.3267	187.1	11928.4	23539.4	2462.3	1.1	2.5	11.9	1.1	3.5	15.4	184.0	AK
17	MOUNT OLIVE	5.6267	7.3370	191.8	734.6	31032.5	1249.0	2.5	5.4	405.9	2.5	7.9	413.8	179.0	AK
18	UMUANUNU	5.6322	7.3403	322.4	2214.7	8442.1	3060.4	1.5	31.3	64.4	1.5	32.8	97.2	159.0	AK
19	UMUDIMIRE	5.6508	7.3281	3860.5	311.9	43.9	235.3	0.9	14.0	11.2	0.9	14.9	26.1	168.0	QH
20	EZEOKE	5.5436	7.3600	5276.1	418.8	468.9	1880.8	1.0	7.7	41.6	1.0	8.6	50.2	115.0	HA
21	UMUEZEALA	5.6264	7.3494	588.2	12.8	252.4	760.5	0.7	1.0	32.2	0.7	1.7	33.9	171.0	HA
22	NDI OWERRE	5.6281	7.3440	1974.7	9519.1	977.7	30801.2	4.4	7.7	38.1	4.4	12.1	40.2	189.0	KA
23	UMUEHIE DURUODU	5.6294	7.3303	116.7	6731.2	11593.1	1563.3	1.3	3.1	19.6	1.3	4.3	23.9	169.0	AK
24	UMUAKAGU	5.6289	7.3186	76.7	4456.1	2400.6	2444.6	0.9	5.4	38.2	0.9	6.3	44.6	168.0	KH
25	IGBO IHITTE	5.6206	7.3136	128.2	2347.9	55779.1	17521.1	1.6	1.7	22.0	1.6	3.3	25.3	129.0	AK
26	UMUIKE LOWA	5.6339	7.3527	1776.4	2025.3	10188.6	1774.2	2.1	7.2	15.4	2.1	9.3	24.7	162.0	AK
27	UMUDIEBELE	5.6411	7.3638	1746.2	111.9	346.7	104.2	0.7	20.4	80.3	0.7	21.1	101.4	105.0	HK
28	UMU-UDO	5.6517	7.3851	1123.6	201.6	7721.1	461.2	1.2	5.5	48.2	1.2	6.7	54.9	125.0	HK
29	UMUNUMO-UBOMA	5.6466	7.3925	1341.1	172.4	1678.8	304.3	1.4	2.6	8.2	1.4	3.9	12.1	101.0	HK
30	UZINOMI	5.6470	7.3608	329.1	441.6	8.3	90.5	3.4	4.3	80.7	3.4	7.7	88.4	93.0	KH
31	UMUCHAKU	5.6489	7.3560	459.9	159.5	1194.1	57.5	5.9	24.4	60.4	5.9	30.3	90.7	120.0	HK
32	UMUHI 1	5.6142	7.3611	198.3	3455.8	5574.4	626.9	1.6	34.1	61.1	1.6	37.0	98.1	161.0	AK
33	UMUIHI II	5.6007	7.3506	745.0	2947.4	11697.7	6489.6	1.0	19.7	110.5	1.0	20.6	131.1	158.0	AK

Table 5 – Summary of Interpreted Vertical Electrical Sounding (VES) Data — Continued

VES	Location	Latitude (°N)	Longitude (°E)	Layer resistivity (Ωm)				Thickness (m)			Depth (m)			Elevation (m)	Curve Types
				ρ_1	ρ_2	ρ_3	ρ_4	h_1	h_2	h_3	d_1	d_2	d_3		
34	UMUAWUCHI II	5.6120	7.3556	4558.4	152.1	9521.3	728.5	0.5	13.6	81.9	0.5	14.1	96.0	164.0	HK
35	UMUDERIM	5.6029	7.3632	979.8	1345.5	4300.1	1001.9	2.2	18.4	50.2	2.2	20.7	70.8	157.0	AK
36	AMAINYI-NTA	5.6002	7.3688	306.9	1301.6	816.5	4890.3	1.4	5.2	9.3	1.4	6.6	15.9	146.0	KH
37	EKWEREOCHA	5.6162	7.3341	267.2	221.9	4611.1	326.9	5.2	9.0	37.1	5.2	14.2	51.4	163.0	HK
38	ABUEKE	5.6092	7.3786	500.4	3791.2	4551.9	780.5	1.3	7.9	57.8	1.3	9.2	67.0	126.0	AK
39	UMUOYO	5.6140	7.3930	735.3	114.0	598.6	787.4	1.5	20.0	132.6	1.5	21.5	154.1	130.0	HA
40	IKPEREJERE	5.6274	7.3749	224.7	72.2	25.8	584.5	2.5	4.8	40.3	2.5	7.3	47.6	118.0	QH
41	UMUOKORO	5.6265	7.3900	873.2	2522.7	1275.4	6853.5	2.9	5.8	12.4	2.9	8.8	21.2	159.0	KH
42	NDIOWERE-UMUIKE	5.6346	7.3597	179.2	695.5	252.4	315.9	0.9	2.0	22.0	0.9	2.9	24.9	115.0	KH
43	AMAINYI-UKWU	5.6655	7.3028	868.8	197.7	3490.3	971.4	6.3	9.6	37.1	6.3	15.9	53.0	123.0	HK
44	NKWUMATO	5.6293	7.3924	621.8	40.8	658.0	398.5	2.5	5.5	8.4	2.5	8.0	16.4	116.0	HK
45	IKPEREJERE II	5.6286	7.3610	22.2	97.1	3224.6	510.5	3.7	1.9	36.1	3.7	5.5	41.6	119.0	AK
46	UMUDERIM II	5.6810	7.3541	94.3	628.6	3530.8	422.9	3.0	2.3	24.1	3.0	5.3	29.4	122.0	AK
47	UMUDOMA	5.6661	7.5365	87.8	65.9	108.0	2792.1	2.1	11.8	20.1	2.1	13.9	34.1	115.0	HA
48	ONICHA-UBOMA	5.6428	7.3766	86.2	601.9	662.3	101.2	0.9	26.6	67.4	0.9	27.4	94.8	131.0	AK
49	UMUOBIKE	5.6184	7.4147	282.1	1907.4	6264.8	10611.9	2.3	3.1	72.6	2.3	5.4	78.0	113.0	AA
50	ABUEKE II	5.6313	7.3613	125.6	30.5	2430.8	12.5	2.0	3.0	23.0	2.0	4.9	27.9	118.0	HK

VES curve types (KH, HK, H, AK, KA, QH, KQ, HA, AA) indicate subsurface variability. KH-type curves dominate, representing a resistive top layer, conductive middle aquifer, and resistive base—favorable for groundwater storage. HK and H-types also highlight aquifer potential, while less common types (e.g., AK, KA) suggest complex stratigraphy or confined aquifers.

4.2. Aquifer Vulnerability Index (AVI)

The Aquifer Vulnerability Index (AVI) quantifies susceptibility to contamination by evaluating the hydraulic resistance of the overlying vadose zone. Locations with low AVI values correspond to minimal protective cover and high contamination risk. Most locations (e.g., UMUOKE, UMUARIAM II, MOUNT OLIVE) exhibited extremely high vulnerability, reflecting highly permeable vadose zones. A smaller group demonstrated low to moderate vulnerability (e.g., EHUME, OKWUOHIA), where the vadose zone provides limited natural protection (Table 6). This pattern is consistent with recent groundwater vulnerability assessments that integrate index-based models with hydrogeophysical and water quality analyses (Ahmed; Kumar; Singh, 2022; Kumar *et al*., 2023; Singh; Sharma; Patel, 2023).

Table 6 – Interpreted Summary of Aquifer Vulnerability Index

Locations	ρ_1 (Ωm)	ρ_2 (Ωm)	ρ_3 (Ωm)	C	Log_{10} C	Vulnerability
EHUME	1178.1	221.1	2926.7	4325.9	3.64	Low
OKWUOHIA	477.2	1174.3	1783.4	3434.9	3.54	Low
UMUARIAM	110.5	4538.2	119	4767.7	3.68	Low
UMULOGHO	350.5	987.3	5637.9	6975.7	3.84	Low
UMUOKE	1683.9	1139.6	245	3068.5	3.49	Low
ACHARA	201.4	37.8	158.5	397.7	2.6	Moderate
ALIKE	326.1	315	1338.1	1979.2	3.3	Low
AMANZE	67.5	1359.1	288.9	1715.5	3.23	Low
AMUZI	192.7	167.6	825.6	1185.9	3.07	Low
AVUTU	374.5	1318.4	3081.6	4774.5	3.68	Low
UMUSOCHIE	332	37.3	2285.4	2654.7	3.42	Low
ODENKUME	379.4	1275.8	934.3	2589.5	3.41	Low
OKWUOHIA II	307.2	51.4	278.4	637	2.8	Moderate
UMUNACHI	172.7	627.1	6192.8	6992.6	3.84	Low
UMUARIAM2	998	4228.7	2501.2	7727.9	3.89	Low
UMUAKAGU II	187.1	11928.4	23539.4	35654.9	4.55	Extremely low
MOUNT OLIVE	191.8	734.6	31032.5	31959	4.5	Extremely low
UMUANUNU	322.4	2214.7	8442.1	10979.2	4.04	Extremely low
UMUDIMIRE	3860.5	311.9	43.9	4216.3	3.63	Low
EZEOKE	5276.1	418.8	468.9	6163.8	3.79	Low
UMUEZEALA	588.2	12.8	252.4	853.4	2.93	Moderate
NDI OWERRE	1974.7	9519.1	977.7	12471.5	4.1	Extremely low
UMUEHIE DURUODU	116.7	6731.2	11593.1	18441	4.27	Extremely low
UMUAKAGU	76.7	4456.1	2400.6	6933.4	3.84	Low
IGBO IHITTE	128.2	2347.9	55779.1	58255.2	4.77	Extremely low
UMUIKE LOWA	1776.4	2025.3	10188.6	13990.3	4.15	Extremely low
UMUDIEBELE	1746.2	111.9	346.7	2204.8	3.34	Low
UMU-UDO	1123.6	201.6	7721.1	9046.3	3.96	Low
UMUNUMO-UBOMA	1341.1	172.4	1678.8	3192.3	3.5	Low
UZINOMI	329.1	441.6	8.3	779	2.89	Moderate
UMUCHAKU	459.9	159.5	1194.1	1813.5	3.26	Low
UMUHI 1	198.3	3455.8	5574.4	9228.5	3.97	Low
UMUIHI II	745	2947.4	11697.7	15390.1	4.19	Extremely low
UMUAWUCHI II	4558.4	152.1	9521.3	14231.8	4.15	Extremely low
UMUDERIM	979.8	1345.5	4300.1	6625.4	3.82	Low
AMAINYI-NTA	306.9	1301.6	816.5	2425	3.38	Low
EKWEREOCHA	267.2	221.9	4611.1	5100.2	3.71	Low
ABUEKE	500.4	3791.2	4551.9	8843.5	3.95	Low
UMUOYO	735.3	114	598.6	1447.9	3.16	Low
IKPEREJERE	224.7	72.2	25.8	322.7	2.51	Moderate
UMUOKORO	873.2	2522.7	1275.4	4671.3	3.67	Low
NDIOWERE-UMUIKE	179.2	695.5	252.4	1127.1	3.05	Moderate
AMAINYI-UKWU	868.8	197.7	3490.3	4556.8	3.66	Low
NKWUMATO	621.8	40.8	658	1320.6	3.12	Low

Table 6 – Interpreted Summary of Aquifer Vulnerability Index — Continued

Locations	ρ_1 (Ωm)	ρ_2 (Ωm)	ρ_3 (Ωm)	C	Log_{10} C	Vulnerability
IKPEREJERE II	22.2	97.1	3224.6	3343.9	3.52	Low
UMUDERIM II	94.3	628.6	3530.8	4253.7	3.63	Low
UMUDOMA	87.8	65.9	108	261.7	2.42	Moderate
ONICHA-UBOMA	86.2	601.9	662.3	1350.4	3.13	Low
UMUOBIKE	282.1	1907.4	6264.8	8454.3	3.93	Low
ABUEKE II	125.6	30.5	2430.8	2586.9	3.41	Low

Contour maps (Fig. 4) highlight high-risk areas (UMUOKE, ACHARA, AVUTU) with low AVI values, indicating shallow aquifers and limited filtration. These zones require stringent protection measures to prevent pollutant migration.

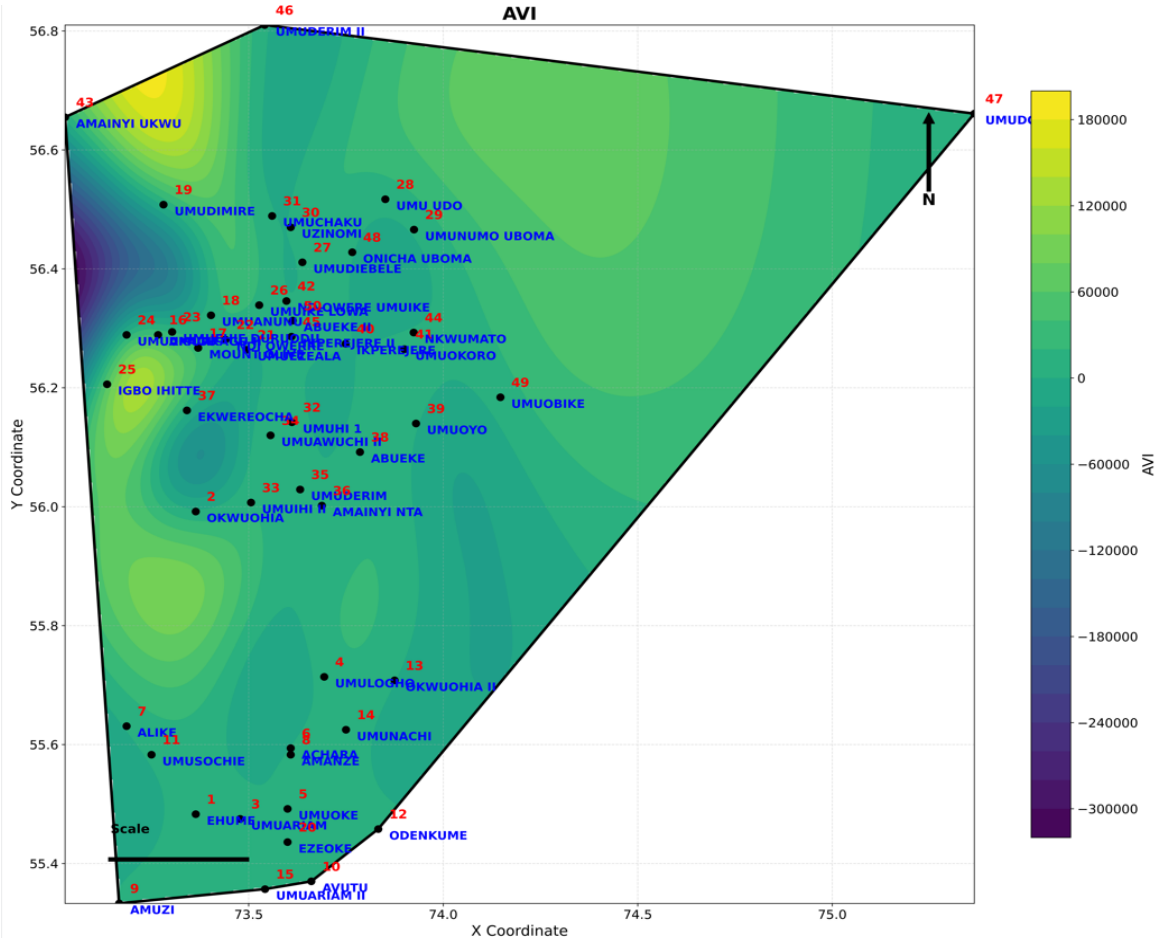

Figure 3. Aquifer Vulnerability Index Contour Map.

4.3. DRASTIC Model

The **DRASTIC model** was applied at 50 VES locations, considering depth to water table (D), recharge (R), aquifer media (A), soil media (S), topography (T), impact of the vadose zone (I), and hydraulic conductivity (C). Parameters were derived from geoelectric data and regional hydrogeological information (Egor, 2022; Nwankwoala; Okujagu, 2014; Babagana; Sharma, 2021; Okorie; Ibuot; George, 2017; Olayinka, 1996). DRASTIC index values ranged from 105 to 155 (Table 7). Locations like UMUOKE, ACHARA, and UMUEZEALA exhibited very high vulnerability (≥150), while VES 4 (UMULOGHO), VES 8 (AMANZE), and VES 11 (UMUSOCHIE) showed moderate vulnerability. Low-risk sites (≤120) included VES 13, 15, 16, and 17.

Contour mapping (Fig. 5) identifies critical zones for targeted groundwater management. High DRASTIC values correlate with shallow water tables, permeable soils, and flat terrain, increasing pollutant infiltration potential.

Table 7 – Summary of DRASTIC Model Interpretation

VES	Location	D (×5)	R (6×4)	A (×3)	S (7×2)	T (9×1)	I (×5)	C (×5)	DRASTIC Index
VES 1	**EHUME**	25	24	3	14	9	35	35	145
VES 2	**OKWUOHIA**	25	24	9	14	9	25	35	141
VES 3	**UMUARIAM**	35	24	3	14	9	15	35	135
VES 4	**UMULOGHO**	25	24	3	14	9	25	25	125
VES 5	**UMUOKE**	50	24	3	14	9	35	15	150
VES 6	**ACHARA**	35	24	9	14	9	25	35	151
VES 7	**ALIKE**	25	24	3	14	9	35	35	145
VES 8	**AMANZE**	25	24	21	14	9	25	5	123
VES 9	**AMUZI**	35	24	3	14	9	15	35	135
VES 10	**AVUTU**	50	24	9	14	9	25	15	146
VES 11	**UMUSOCHIE**	25	24	3	14	9	25	25	125
VES 12	**ODENKUME**	25	24	3	14	9	15	35	125
VES 13	**OKWUOHIA II**	25	24	3	14	9	15	15	105
VES 14	**UMUNACHI**	25	24	3	14	9	25	25	125
VES 15	**UMUARIAM II**	25	24	3	14	9	15	15	105
VES 16	**UMUAKAGU II**	25	24	3	14	9	15	15	105
VES 17	**MOUNT OLIVE**	25	24	3	14	9	15	15	105
VES 18	**UMUANUNU**	25	24	3	14	9	25	25	125
VES 19	**UMUDIMIRE**	25	24	3	14	9	15	15	105
VES 20	**EZEOKE**	25	24	3	14	9	25	25	125
VES 21	**UMUEZEALA**	35	24	3	14	9	35	35	155
VES 22	**NDI OWERRE**	25	24	3	14	9	15	15	105
VES 23	**UMUEHIE DURUODU**	25	24	3	14	9	25	25	125
VES 24	**UMUAKAGU**	25	24	3	14	9	15	15	105
VES 25	**IGBO IHITTE**	25	24	3	14	9	25	25	125
VES 26	**UMUIKE LOWA**	25	24	3	14	9	25	25	125
VES 27	**UMUDIEBELE**	25	24	3	14	9	15	15	105
VES 28	**UMU-UDO**	25	24	3	14	9	25	25	125
VES 29	**UMUNUMO-UBOMA**	25	24	3	14	9	15	15	105
VES 30	**UZINOMI**	25	24	3	14	9	25	25	125
VES 31	**UMUCHAKU**	25	24	3	14	9	25	25	125
VES 32	**UMUHI 1**	35	24	3	14	9	25	25	135
VES 33	**UMUIHI 2**	25	24	3	14	9	25	25	125
VES 34	**UMUAWUCHI 2**	25	24	3	14	9	25	25	125
VES 35	**UMUDERIM**	25	24	3	14	9	15	15	105
VES 36	**AMAINYI-NTA**	25	24	3	14	9	15	15	105
VES 37	**EKWEREOCHA**	25	24	3	14	9	15	15	105
VES 38	**ABUEKE**	25	24	3	14	9	15	15	105
VES 39	**UMUOYO**	25	24	3	14	9	15	15	105
VES 40	**IKPEREJERE**	25	24	3	14	9	15	15	105
VES 41	**UMUOKORO**	25	24	3	14	9	25	25	125
VES 42	**NDIOWERE-UMUIKE**	25	24	3	14	9	25	25	125
VES 43	**AMAINYI-UKWU**	25	24	3	14	9	25	25	125
VES 44	**NKWUMATO**	25	24	3	14	9	15	15	105
VES 45	**IKPEREJERE II**	25	24	3	14	9	25	25	125
VES 46	**UMUDERIM II**	25	24	3	14	9	15	15	105
VES 47	**UMUDOMA**	25	24	3	14	9	15	15	105
VES 48	**ONICHA-UBOMA**	35	24	3	14	9	25	25	135
VES 49	**UMUOBIKE**	25	24	3	14	9	25	25	125
VES 50	**ABUEKE II**	25	24	3	14	9	15	15	105

4.4. SINTACS Model

The **SINTACS model** uses the same seven parameters as DRASTIC but applies a dynamic weighting system to reflect local hydrogeological sensitivity. Parameters (S, I, N, T, A, C, S) were derived from geoelectric data, regional recharge, and soil characteristics. SINTACS indices ranged from 105 to 186 (Table 8). Low vulnerability sites (105) included OKWUOHIA, AVUTU, UMUARIAM II, and UMUIKE LOWA. Moderate indices (110–123) occurred at VES 1 (EHUME) and VES 4 (UMULOGHO). High vulnerability was observed at ACHARA, UMUSOCHIE, and UMUEZEALA, while very high vulnerability zones (≥171) included UMUDIMIRE, UZINOMI, and IKPEREJERE.

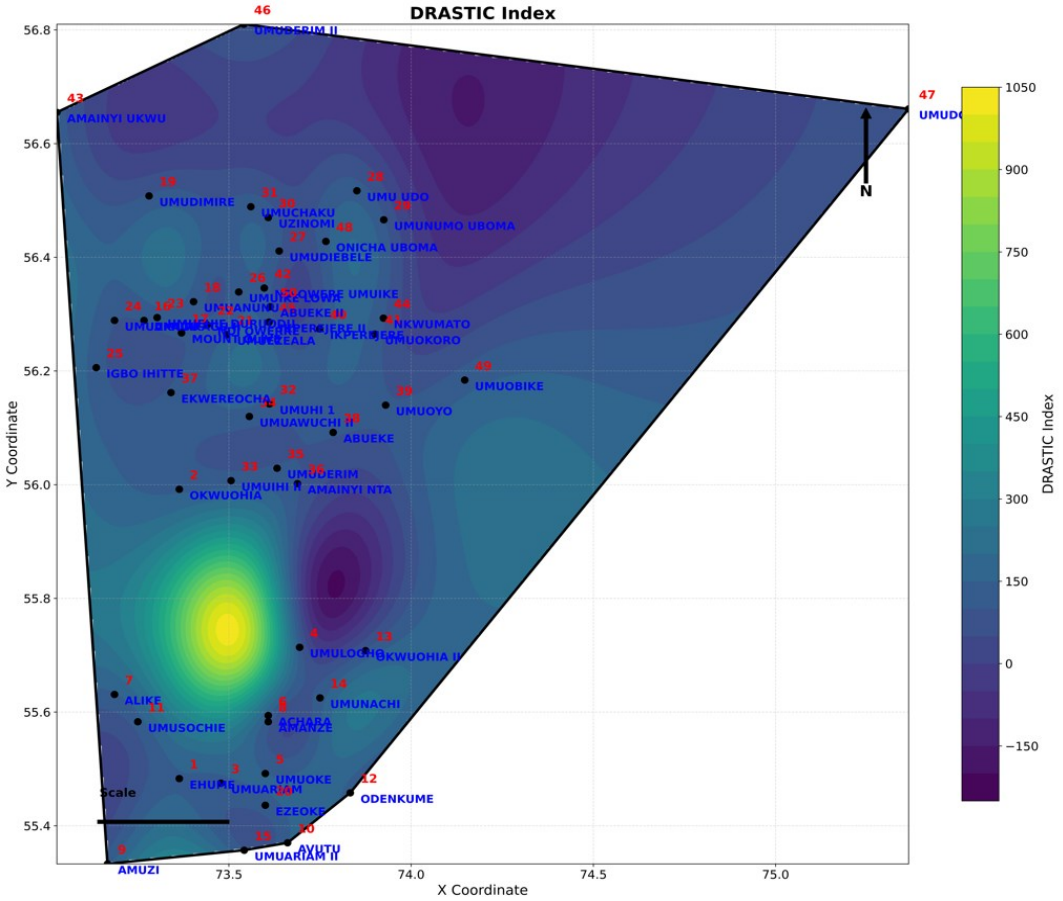

Figure 4. DRASTIC Contour Map.

Contour maps (Fig. 6) reveal elevated pollution potential in UMUARIAM, ACHARA, and MOUNT OLIVE, aligning with field observations of anthropogenic impact.

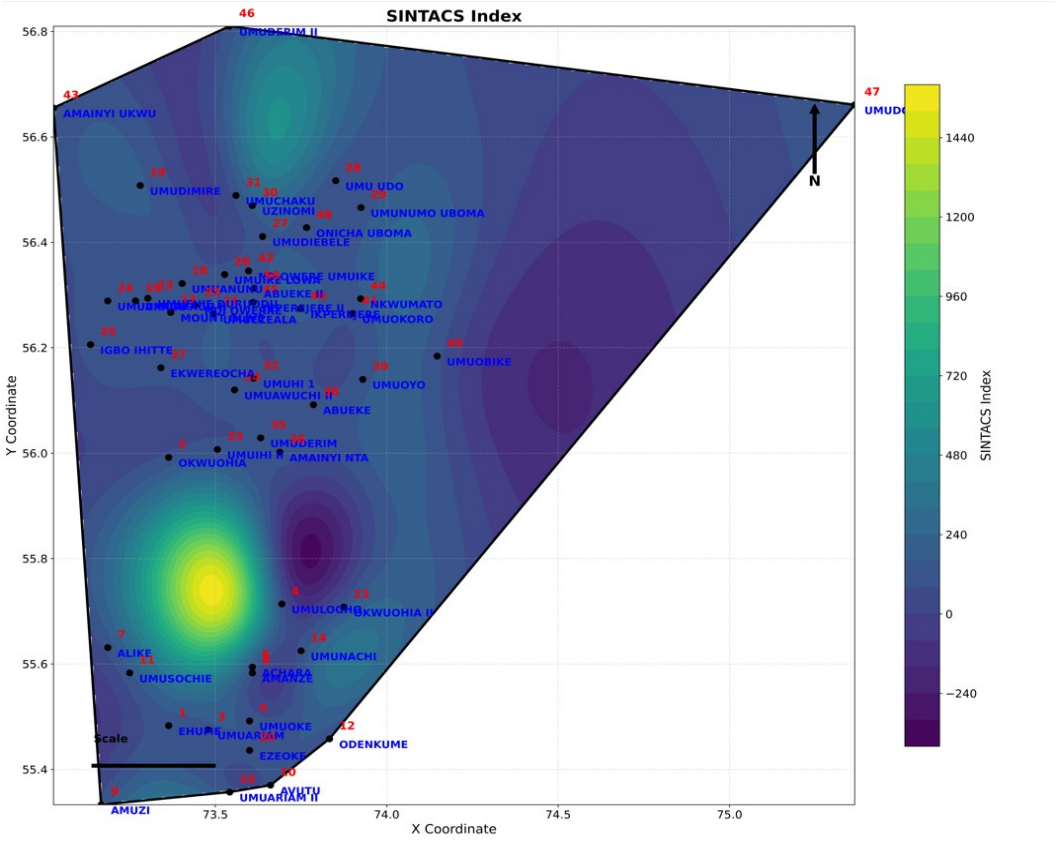

Figure 5. SINTACS Contour Map.

Table 8 – Summary of SINTACS Model

VES	Location	S(RxW)	I(RxW)	N(RxW)	T(RxW)	A(RxW)	C(RxW)	S(RxW)	SINTACS Index
1	EHUME	45	24	3	14	9	20	5	120
2	OKWUOHIA	45	24	3	14	9	5	5	105
3	UMUARIAM	50	24	12	14	9	5	20	134
4	UMULOGHO	45	24	3	14	9	10	5	110
5	UMUOKE	45	24	12	14	9	5	20	129
6	ACHARA	45	24	12	14	9	40	20	164
7	ALIKE	45	24	3	14	9	10	5	110
8	AMANZE	45	24	6	14	9	5	10	113
9	AMUZI	45	24	6	14	9	20	10	128
10	AVUTU	45	24	3	14	9	5	5	105
11	UMUSOCHIE	50	24	3	14	9	40	5	145
12	ODENKUME	45	24	6	14	9	5	10	113
13	OKWUOHIA II	45	24	6	14	9	30	10	138
14	UMUNACHI	45	24	3	14	9	10	5	110
15	UMUARIAM II	45	24	3	14	9	5	5	105
16	UMUAKAGU II	45	24	3	14	9	5	5	105
17	MOUNT OLIVE	45	24	3	14	9	10	5	110
18	UMUANUNU	45	24	3	14	9	5	5	105
19	UMUDIMIRE	50	24	24	14	9	10	40	171
20	EZEOKE	50	24	6	14	9	10	10	123
21	UMUEZEALA	50	24	6	14	9	40	10	153
22	NDI OWERRE	45	24	6	14	9	5	10	113
23	UMUEHIE DURUODU	45	24	3	14	9	5	5	105
24	UMUAKAGU	50	24	3	14	9	5	5	110
25	IGBO IHITTE	45	24	3	14	9	5	5	105
26	UMUIKE LOWA	45	24	3	14	9	5	5	105
27	UMUDIEBELE	50	24	6	14	9	20	10	133
28	UMU-UDO	45	24	3	14	9	20	5	120
29	UMUNUMO-UBOMA	45	24	3	14	9	20	5	120
30	UZINOMI	45	24	30	14	9	10	50	182
31	UMUCHAKU	35	24	3	14	9	20	5	110
32	UMUHI 1	45	24	3	14	9	5	5	105
33	UMUIHI II	50	24	3	14	9	5	5	110
34	UMUAWUCHI 2	50	24	3	14	9	20	5	125
35	UMUDERIM	45	24	3	14	9	5	5	105
36	AMAINYI-NTA	45	24	6	14	9	5	10	113
37	EKWEREOCHA	35	24	3	14	9	20	5	110
38	ABUEKE	45	24	3	14	9	5	5	105
39	UMUOYO	45	24	6	14	9	20	10	128
40	IKPEREJERE	45	24	24	14	9	30	40	186
41	UMUOKORO	45	24	3	14	9	5	5	105
42	NDIOWERE-UMUIKE	50	24	6	14	9	10	10	123
43	AMAINYI-UKWU	35	24	3	14	9	20	5	110
44	NKWUMATO	45	24	6	14	9	40	10	148
45	IKPEREJERE II	45	24	3	14	9	30	5	130
46	UMUDERIM II	45	24	3	14	9	10	5	110
47	UMUDOMA	45	24	12	14	9	30	20	154
48	ONICHA-UBOMA	50	24	6	14	9	10	10	123
49	UMUOBIKE	45	24	3	14	9	5	5	105
50	ABUEKE II	45	24	3	14	9	40	5	140

4.5. Comparison of DRASTIC vs SINTACS Indices

Both indices identify groundwater vulnerability but differ in sensitivity. DRASTIC provides a generalized overview, whereas SINTACS captures localized variability. The SINTACS Index (105–186) exhibits a broader range than DRASTIC (105–155), reflecting its responsiveness to local hydrogeology, land use, and aquifer properties (Fig. 7). Sites such as UMUOKE, UMUANUNU, UMUNUMO-UBOMA, and UMUOYO show significantly higher SINTACS values, emphasizing higher vulnerability not fully captured by DRASTIC.

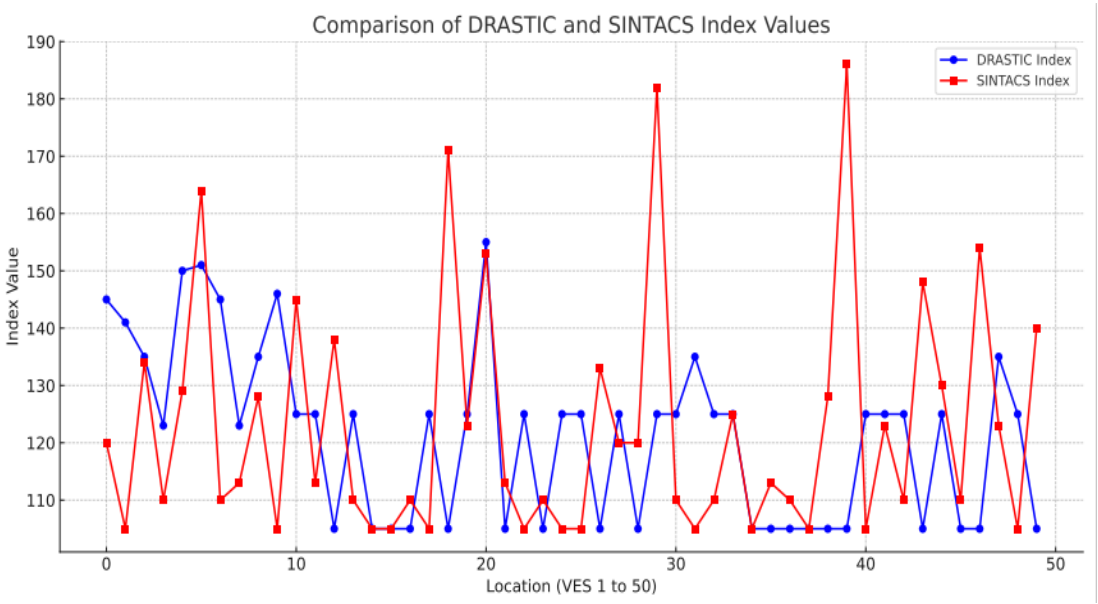

Figure 6. Comparison of DRASTIC and SINTACS Index Value.

Using both models provide complementary insights: DRASTIC for regional-scale planning, and SINTACS for detailed, site-specific risk assessment.

4.6. Water Quality Index (WQI)

The Water Quality Index (WQI) was used to evaluate the overall groundwater quality in the study area based on selected physicochemical and biological parameters, following the classification of Brown *et al.* (1970). The calculated WQI values (Table 9) show spatial variability in groundwater quality across the study locations. The lowest WQI value (40.22) was recorded at UMUIKE LOWA, indicating *Good* water quality. In contrast, UMUANUNU (50.39), MOUNT OLIVE (50.43), EZEOKE (52.03), and UMU-UDO (63.38) fall within the *Poor* water quality category, suggesting moderate degradation and limited suitability for direct consumption without treatment. Higher WQI values were observed in UMULOGHO (76.63), UMUARIAM (76.78), and OKWUOHIA (77.27), classifying groundwater in these areas as Very Poor. The elevated WQI values are mainly attributed to increased biological oxygen demand, indicating possible organic contamination.

Table 8 – Summary of SINTACS Model

Location	WQI	Water Quality
UMUIKE LOWA	40.22	Good
UMUANUNU	50.39	Poor
MOUNT OLIVE	50.43	Poor
EZEOKE	52.03	Poor
UMU-UDO	63.38	Poor
UMULOGHO	76.63	Very Poor
UMUARIAM	76.78	Very Poor
OKWUOHIA	77.27	Very Poor

The spatial distribution of WQI (Figure 8) reveals a general decline in groundwater quality toward the Obowo axis of the study area. This pattern corresponds well with the AVI, DRASTIC, and SINTACS vulnerability maps, where areas of higher aquifer vulnerability coincide with poorer water quality. The WQI results therefore provide hydrochemical validation of the vulnerability models and highlight areas where groundwater protection and treatment measures are required.

4.7. Broader implications for groundwater management and policy

Although this study focuses on Okigwe South in southeastern Nigeria, the findings have broader implications for groundwater management in regions characterized by similar hydrogeological, climatic, and socio-economic conditions. Many parts of sub-Saharan Africa and other developing regions rely heavily on shallow groundwater

systems for domestic and agricultural use, often with limited regulatory oversight and minimal natural protection of aquifers. The dominance of high to extremely high vulnerability classes identified using the AVI, DRASTIC, and SINTACS models highlights a critical challenge common to many sedimentary basins worldwide, where permeable vadose zones and shallow water tables facilitate rapid contaminant migration. The convergence of results from multiple index-based models strengthens confidence in the identification of pollution-prone zones and demonstrates the robustness of integrating geophysical data with vulnerability assessment frameworks. This multi-model agreement suggests that the applied methodology is transferable to other data-scarce regions where detailed hydrogeological or geochemical datasets are unavailable. In such settings, electrical resistivity surveys combined with standardized vulnerability indices provide a cost-effective and defensible approach for preliminary groundwater protection planning.

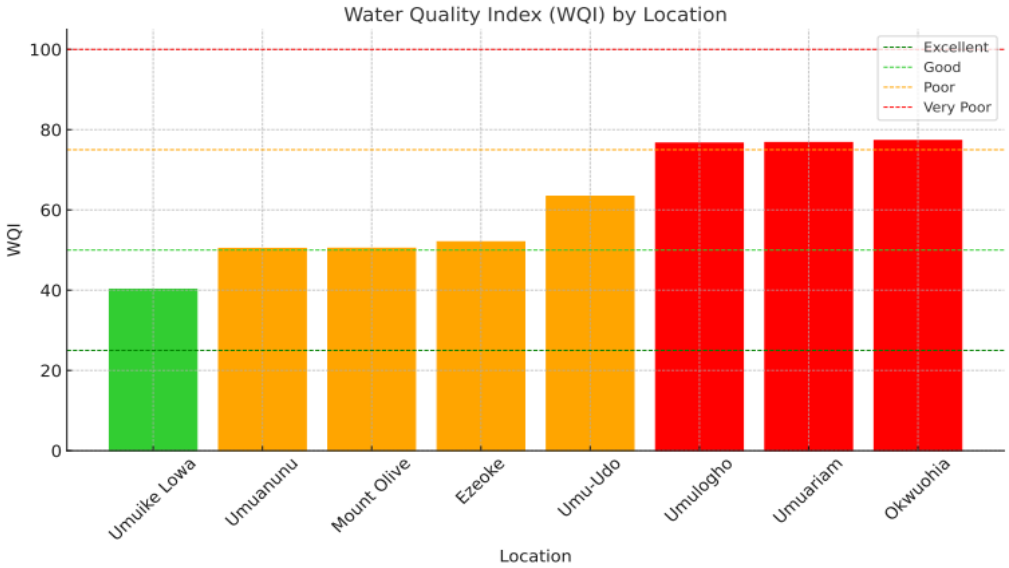

Figure 7. Location of Water Quality Index.

From a management perspective, the spatial patterns of vulnerability revealed in this study offer a practical decision-support tool for land-use planning, borehole siting, and pollution control. Areas consistently classified as highly vulnerable should be prioritized for stricter regulation of waste disposal, agricultural chemical application, and groundwater abstraction. Conversely, zones with relatively lower vulnerability may be better suited for controlled groundwater development, provided that routine monitoring is maintained.

At a broader scale, the study underscores the importance of preventive groundwater management rather than reactive remediation, which is often economically unfeasible in developing regions. By identifying vulnerable aquifers before severe contamination occurs, index-based vulnerability mapping supports proactive protection strategies aligned with global sustainable development goals, particularly those related to clean water access and environmental protection. Consequently, the approach and findings presented here contribute to the growing body of international research advocating vulnerability assessment as a foundational component of sustainable groundwater resource management.

5. CONCLUSION

This study employed an integrated geophysical, hydrogeological, and hydrochemical framework to evaluate aquifer vulnerability and groundwater quality in Okigwe South, southeastern Nigeria. The combined application of AVI, DRASTIC, and SINTACS models, supported by vertical electrical sounding data and water quality analysis, proved effective in delineating spatial variations in aquifer susceptibility to contamination. Results show that areas underlain by highly permeable sandy formations, shallow groundwater levels, and thin protective layers exhibit moderate to very high vulnerability, particularly within Obowo LGA. The Water Quality Index corroborates these findings, with poorer groundwater quality observed in zones identified as highly vulnerable by the vulnerability models. This agreement highlights the reliability of the integrated approach and confirms the influence of both natural hydrogeological conditions and anthropogenic activities on groundwater integrity.

Although index-based models involve inherent simplifications and uncertainties, their integration with geophysical and hydrochemical data significantly improves assessment confidence. The vulnerability and water quality maps generated in this study provide practical tools for groundwater protection zoning, monitoring, and land-use planning. It is recommended that high-risk zones receive priority attention in groundwater management policies, including controlled waste disposal, regulation of agricultural practices, and periodic water quality monitoring to safeguard public health and ensure sustainable groundwater use.

ACKNOWLEDGEMENTS

This research was independently conducted by the authors through collaborative effort in fieldwork, data analysis, and manuscript preparation. The authors gratefully acknowledge the support provided by the **Department of Physics and Astronomy, University of Nigeria, Nsukka**, for facilitating access to academic resources and technical guidance throughout the course of this study.

REFERENCES

AGOUBI, B.; KHARROUBI, A.; ABIDA, H. Assessment of groundwater vulnerability to pollution using intrinsic vulnerability methods. **Environmental Earth Sciences**, [*s. l.*], v. 77, n. 9, Article 315, 2018.

AHMED, S.; KUMAR, P.; SINGH, R. Groundwater vulnerability and water quality assessment using integrated approaches. **Water Supply**, [*s. l.*], v. 22, n. 6, p. 5123–5137, 2022. DOI: https://doi.org/10.2166/ws.2022.126.

AKPAN, A. E.; ILORI, A. O.; ESSIEN, N. U. Geoelectric investigation of groundwater potential in crystalline basement terrains. **Journal of African Earth Sciences**, [*s. l.*], v. 87, p. 56–66, 2013. DOI: https://doi.org/10.1016/j.jafrearsci.2013.07.003.

ALLER, L.; BENNETT, T.; LEHR, J. H.; PETTY, R. J.; HACKETt, G. **DRASTIC:** A standardized system for evaluating groundwater pollution potential using hydrogeologic settings (EPA/600/2-87/035). U.S. Ada: Environmental Protection Agency, 1987

ANYANWU, C. N.; OGUNTADE, O. Stratigraphic and sedimentological characteristics of the Imo Formation, southeastern Nigeria. **Journal of African Earth Sciences**, [*s. l.*], v. 73, 104040. 2021.

AWAWDEH, M.; AL-MAHAMID, J.; JARADAT, R. Groundwater vulnerability assessment using the SINTACS model. **Environmental Monitoring and Assessment**, [*s. l.*], v. 192, n. 4, 255, 2020.

BABAGANA, A.; SHARMA, A. Assessment of groundwater vulnerability to contamination using index models. **Environmental Monitoring and Assessment**, [*s. l.*], v. 193, n. 6, Article 352. 2021. DOI: https://doi.org/10.1007/s10661-021-09065-4

BROWN, R. M.; MCCLELLAND, N. I.; DEININGER, R. A.; O'CONNOR, M. F. A water quality index—Crashing the psychological barrier. *In*: DAVIS, W. S. (ed.). **Indicators of environmental quality**. New York: Plenum Press, 1970. p. 173–182

CHRISTENSEN, T. (ed.). **Solid waste technology and management.** Hoboken: John Wiley & Sons, 2011.

CIVITA, M. **Le carte della vulnerabilità degli acquiferi all'inquinamento**. Bologna: Pitagora Editrice, 1994

CIVITA, M.; DE MAIO, M. **SINTACS R5:** A new parametric system for groundwater vulnerability assessment. Bologna: Pitagora Editrice, 1997.

DUCCI, D.; SELLERINO, M. Vulnerability mapping of groundwater. **Journal of Environmental Management**, [*s. l.*], v. 122, p. 45–53, 2013. DOI: https://doi.org/10.1016/j.jenvman.2013.02.002

EGOR, A. O. Groundwater vulnerability assessment using index-based models in sedimentary basins. **Environmental Earth Sciences**, [*s. l.*], v. 81, n. 12, Article 345, 2022.

EKANEM, A. M.; UDOSEN, C. Improved resistivity data processing for layered media in groundwater studies. **Environmental Earth Sciences**, [*s. l.*], v. 82, n. 3, Article 136, 2023a.

EKANEM, A. M.; UDOSEN, C. Reducing inversion errors in resistivity interpretation methods. **Journal of African Earth Sciences**, [*s. l.*], v. 196, Article 104737, 2023b.

UNITED STATES. Environmental Protection Agency. Office of Ground Water and Drinking Water. **A review of methods for assessing aquifer sensitivity and ground water vulnerability to pesticide contamination**. Washington, DC: Environmental Protection Agency, 1993.

GEORGE, N. J. Modelling the trends of resistivity gradient in hydrogeological units: a case study of alluvial environment. **Modeling Earth Systems and Environment**, [*s. l.*], v. 7, n. 1, p. 95-104, 2021.

GEORGE, N. J.; IBUOT, J. C.; OBIORA, D. N. Evaluation of aquifer vulnerability using geoelectric and hydrogeological parameters. **Environmental Earth Sciences**, [*s. l.*], v. 80, Article 511, 2021. DOI: https://doi.org/10.1007/s12665-021-09747-6

IBUOT, J. C.; GEORGE, N. J.; OBIORA, D. N. Estimation of aquifer protective capacity using geoelectric parameters. **Journal of African Earth Sciences**, [*s. l.*], v. 87, p. 77–85. 2013. DOI: https://doi.org/10.1016/j.jafrearsci.2013.07.008

JEELANI, G.; SHAH, R. A.; FRYAR, A. E.; DESHPANDE, R. D.; MUKHERJEE, A.; PERRIN, J. Hydrological processes in glacierized high-altitude basins of the western Himalayas. Hydrogeology Journal, v. 26, n. 2, p. 615-628, 2018.

NWAJIDE, C. S. A lithostratigraphic analysis of the Nanka Sands, southeastern Nigeria. **Journal of Mining and Geology**, [*s. l.*], v. 16, p. 103–109, 1979.

NWANKWOALA, H. O.; OKUJAGU, C. U. Assessment of groundwater vulnerability to pollution using DRASTIC model in parts of the Niger Delta, Nigeria. **International Journal of Environmental Science and Technology**, [*s. l.*], v. 11, n. 7, p. 1955–1968. 2014. DOI: https://doi.org/10.1007/s13762-013-0342-9

OBIANWU, V. I.; OKEKE, H. C.; ONYEKURU, S. O. Geoelectric investigation of aquifer characteristics in southeastern Nigeria**.** **Journal of Applied Sciences and Environmental Management**, [*s. l.*], v. 15, n. 2, p. 343–350, 2011.

OKORIE, C. O.; IBUOT, J. C.; GEORGE, N. J. Hydrogeophysical evaluation of aquifer protective capacity in parts of southeastern Nigeria. **Environmental Earth Sciences**, [*s. l.*], v. 76, Article 94, 2017. DOI: https://doi.org/10.1007/s12665-017-6418-2.

OLADIMEJI, O. P.; NWAJIDE, C. S. Sedimentary evolution of the Anambra Basin. **Journal of African Earth Sciences**, [*s. l.*], v. 189, 104458, 2022.

OLAYINKA, A. I. Non-uniqueness in the interpretation of geoelectrical resistivity sounding data. **Journal of Mining and Geology**, [*s. l.*], v. 32, n. 2, p. 221–229, 1996.

OLAYINKA, A. I.; BARKER, R. D. Assessment of groundwater contamination using geoelectrical methods. **Journal of African Earth Sciences**, [*s. l.*], v. 11, n. 1, p. 31–39, 1990.
DOI: https://doi.org/10.1016/0899-5362(90)90019-K

PIVER, W. T.; CHARLES, B.; BARLOW, P. M. Groundwater contamination risks and well abandonment. **Water Resources Research**, [*s. l.*], v. 33, n. 2, p. 271–280, 1997.

SAMPATH, K. Groundwater contamination and well abandonment. **Environmental Geology**, [*s. l.*], v. 39, p. 236–243, 2000.

SHARMA, V.; SINGH, A.; PATEL, R. Aquifer vulnerability mapping using index-based models. **Carbonates and Evaporites**, [*s. l.*], v. 38, n. 2, p. 179–191. 2023. DOI: https://doi.org/10.1007/s12594-023-2347-4

SINGH, A.; SHARMA, V.; PATEL, R. GIS-based groundwater vulnerability analysis using index models. **Sustainable Water Resources Management**, [*s. l.*], v. 9, n. 3, p. 1–14, 2023. DOI: https://doi.org/10.1007/s40808-023-01795-2

VAN STEMPVOORT, D.; EWERT, L.; WASSENAAR, L. Aquifer vulnerability index: A GIS-compatible method for groundwater vulnerability mapping. **Canadian Water Resources Journal**, [*s. l.*], v. 18, n. 1, p. 25–37, 1993. DOI: https://doi.org/10.4296/cwrj1801025

VRBA, J.; ZAPOROZEC, A. **Guidebook on mapping groundwater vulnerability**. [United Kingdom]: International Association of Hydrogeologists, 1994.

VU, T. H.; NGUYEN, H. T.; LE, Q. T. Groundwater vulnerability assessment for sustainable water management. **Environmental Earth Sciences**, [*s. l.*], v. 80, n. 9, Article 392, 2021

ZAPOROZEC, A. **Groundwater vulnerability assessment**. [United Kingdom]: International Association of Hydrogeologists, 1994.